

Unconventional superconductivity originating from disconnected Fermi surfaces in $\text{LaO}_{1-x}\text{F}_x\text{FeAs}$

Kazuhiko Kuroki¹, Seiichiro Onari², Ryotaro Arita³,
Hidetomo Usui¹, Yukio Tanaka², Hiroshi Kontani⁴, and Hideo Aoki⁵

¹ Department of Applied Physics and Chemistry,

The University of Electro-Communications, Chofu, Tokyo 182-8585, Japan

² Department of Applied Physics, Nagoya University, Nagoya 464-8603, Japan and CREST-JST

³ RIKEN, 2-1 Hirosawa, Wako, Saitama 351-0198, Japan

⁴ Department of Physics, Nagoya University, Nagoya 464-8602, Japan and

⁵ Department of Physics, University of Tokyo, Tokyo 113-0033, Japan

(Dated: January 16, 2019)

For a newly discovered iron-based high T_c superconductor $\text{LaO}_{1-x}\text{F}_x\text{FeAs}$, we have constructed a minimal model, where inclusion of all the five d bands is found to be necessary. Random phase approximation is applied to this model to obtain spin and charge susceptibilities, which are then plugged into the linearized Eliashberg equation to investigate the superconductivity. We conclude that the multiple spin fluctuation modes arising from the nesting vectors across and within disconnected Fermi surfaces realizes an unconventional s -wave pairing, where the superconducting gap changes sign across as well as within the Fermi surface pockets.

Understanding the mechanism of unconventional superconductivity has been one of the most challenging problems in condensed matter physics. There is a renewed fascination with a recent discovery of superconductivity in an iron-based superconductor $\text{LaO}_{1-x}\text{F}_x\text{FeAs}$, [1] which is likely to provide a fresh avenue for such a challenge. LaOFeAs belongs to the family of quaternary oxypnictides LnOMPn ($\text{Ln}=\text{La, Pr}$; $\text{M}=\text{Mn, Fe, Co, and Ni}$; $\text{Pn}=\text{P, As}$), which was originally fabricated by Zimmer *et al.* [2, 3] For this family of compounds, Kamihara *et al.* first reported that LaOFeP exhibits superconductivity with $T_c \sim 3\text{K}$, which was subsequently raised to $T_c \sim 7\text{K}$ by F doping. [4] Superconductivity has also been found in Nickel based compounds with the same structure. [5] Very recently, Kamihara *et al.* have come up with the discovery of superconductivity in an arsenide, $\text{LaO}_{1-x}\text{F}_x\text{FeAs}$, where the F doping of $x \simeq 0.11$ leads to a remarkable $T_c \sim 26\text{K}$ (onset $> 30\text{K}$).

The high value of T_c , confirmed also by Chen *et al.* already suggests a possibility of unconventional superconductivity, but direct evidences have been found. A specific heat measurement in magnetic fields shows that the coefficient γ displays a \sqrt{H} behavior. [7] Another measurement, on the point-contact conductance, exhibits spectra with a distinct zero-bias peak, [8] which strongly suggests the presence of sign change in the gap function. [9, 10, 11, 12] The starting material, LaOFeAs , is a bad metal or a semiconductor with some anomaly in the resistivity around 100K . [1] As the system becomes metallic upon F doping, the uniform susceptibility exhibits a Curie-Weiss behavior. Anomalies in the normal-state transport properties have also been reported for the doped system. [13]

Theoretically, first-principles band structure has been obtained for LaOFeP [14], and more recently for LaOFeAs

and related materials [15, 16, 17, 18]. These band structures are metallic with five pieces (sheets) of the Fermi surface in the undoped system, which contradicts with the experiment for the undoped LaOFeAs . [1] However, a dynamical mean field study shows that the electron correlation enhances the crystal field splitting and leads to a band-semiconducting behavior in accord with the experiment. [16] Local spin density calculations for LaOFeAs show that the system is around the border between magnetic and nonmagnetic states, and has a tendency towards ferromagnetism and antiferromagnetism. [15, 17] It is also pointed out that the electron-phonon coupling in this material is not sufficient to account for $T_c = 26\text{K}$. [7, 18]

Given this background, the purpose of the present Letter is to construct a microscopic electronic model for $\text{LaO}_{1-x}\text{F}_x\text{FeAs}$, which should serve as the basis for identifying the possible mechanisms why this material favors high- T_c superconductivity. The minimal model has turned out to contain all the five d orbits, to which we have applied the random phase approximation (RPA) to solve the Eliashberg equation. We shall conclude that a peculiar Fermi surface consisting of multiple pockets and ensuing coexistence of multiple spin-fluctuation modes (nestings in the Fermi surface as indicated by the spin structure peaks) realize a peculiar s -wave pairing, where the superconducting gap changes sign across the inner and the outer Fermi pockets and also within the latter. We also discuss some other possibilities of the gap function.

LaOFeAs has a tetragonal layered structure, in which Fe atoms are arrayed on a square lattice in the form of edge-shared tetrahedra each consisting of Fe surrounded by four As atoms. Due to the tetrahedral coordination there are two Fe atoms per unit cell. Each Fe layer is sandwiched between LaO layers. The experimentally determined lattice constants are $a = 4.03552\text{\AA}$ and

$c = 8.7393\text{\AA}$, and the two internal coordinates are $z_{La} = 0.1415$ and $z_{As} = 0.6512$. We have obtained the band astructure (Fig.1) with the Quantum-ESPRESSO package[19]. We then construct the maximally localized Wannier functions (MLWFs)[20] for the energy window $-2\text{ eV} < \epsilon_k - E_F < 2.6\text{ eV}$, where ϵ_k is the eigenenergy of the Bloch states and E_F the Fermi energy. These MLWFs, centered at the two Fe sites in the unit cell, have five orbital symmetries (orbital 1: $d_{3Z^2-R^2}$, 2: d_{XZ} , 3: d_{YZ} , 4: $d_{X^2-Y^2}$, 5: d_{XY} , where X, Y, Z refer to those for the original unit cell). Since the ten bands are too complicated to deal with, we reduce the model into five-band as follows. We can first note that the two Wannier orbitals in each unit cell are equivalent in that each Fe atom has the same local arrangement of other atoms and that they transform to each other by symmetry operations. We can thus take a unit cell that contains only one orbital per symmetry by unfolding the Brillouin zone (BZ),[21] and we end up with an effective five-band model on a square lattice. x and y axes are then rotated by 45 degrees from X - Y (Fig.2 inset), to which we refer for all the wave vectors hereafter. The in-plane hopping integrals $t(\Delta x, \Delta y, \Delta z = 0; \mu, \nu)$ are displayed in table I, where $[\Delta x, \Delta y]$ is the hopping vector, and μ, ν label the five Wannier orbitals. The on-site energies for the five orbitals are $(\varepsilon_1, \varepsilon_2, \varepsilon_3, \varepsilon_4, \varepsilon_5) = (10.75, 10.96, 10.96, 11.12, 10.62)\text{ eV}$. With these effective hoppings and on-site energies, the in-plane tight-binding Hamiltonian is given in the form

$$H_0 = \sum_{ij} \sum_{\mu\nu} \sum_{\sigma} \left[t(x_i - x_j, y_i - y_j; \mu, \nu) c_{i\mu\sigma}^\dagger c_{j\nu\sigma} + t(x_j - x_i, y_j - y_i; \nu, \mu) c_{j\nu\sigma}^\dagger c_{i\mu\sigma} \right] + \sum_{i\mu\sigma} \varepsilon_\mu n_{i\mu\sigma} \quad (1)$$

where $c_{i\mu\sigma}^\dagger$ creates an electron with spin σ on the μ -th

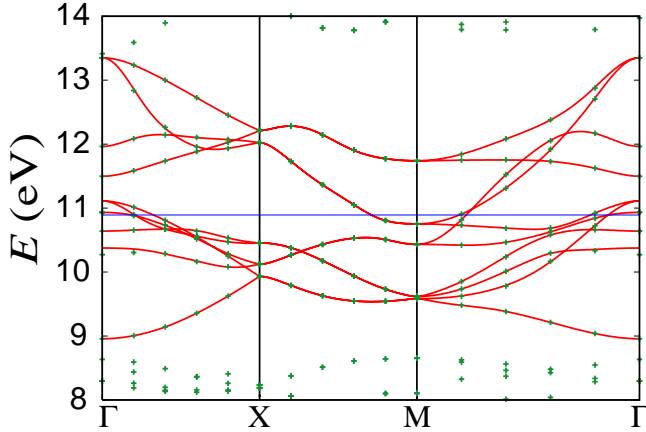


FIG. 1: The band structure of the ten-band model (solid lines) along with the LDA band calculation results (symbols).

orbital at site i , and $n_{i\mu\sigma} = c_{i\mu\sigma}^\dagger c_{i\mu\sigma}$. We define the band filling n as the number of electrons/number of sites (e.g., $n = 10$ for full filling). The doping level x in $\text{LaO}_{1-x}\text{F}_x\text{FeAs}$ is related to the band filling as $n = 6 + x$.

In the obtained band structure in Fig.2(a), we immediately notice that the five bands are heavily entangled, reflecting strong hybridization (see table I) of the five $3d$ orbitals, which is physically due to the tetrahedral coordination of As atoms around Fe. Hence we conclude that the minimal electronic model requires all the five bands.

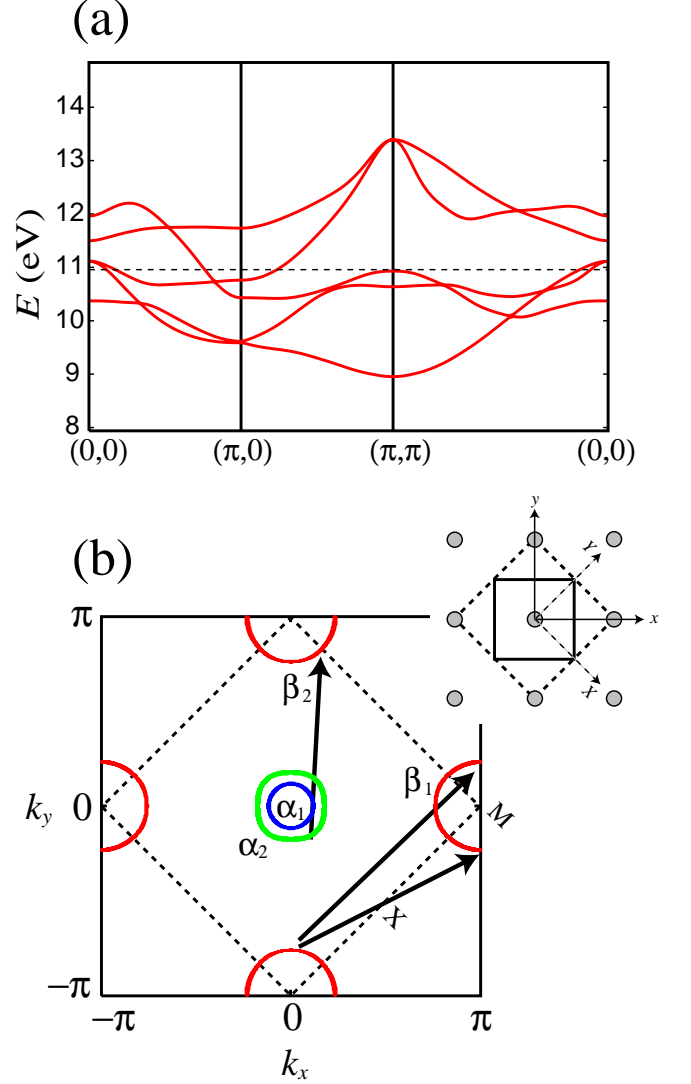


FIG. 2: (a) The band structure of the five-band model in the unfolded BZ, where the inter-layer hoppings are included. To compare with the ten-band model (Fig.1), see the relation between the original and the unfolded BZ shown in figure (b). (b) Fermi surfaces for $n = 6.1$ (with the inter-layer hoppings ignored). Dashed (solid) lines represent the original (unfolded) BZ, while the arrows the nesting vectors. Inset depicts the original (dashed) and reduced (solid) unit cell in real space.

(μ, ν)	[1,0]	[1,1]	[2,0]	[2,1]	[2,2]	σ_y	I	σ_d
(1,1)	-0.7		-0.4	0.2	-0.1	+	+	+
(1,2)	-0.8					-(1,3)	-	-
(1,3)	0.8	-1.5			-0.3	-(1,2)	-	+
(1,4)		1.7			-0.1	-	+	+
(1,5)	-3.0			-0.2		+	+	-
(2,2)	-2.1	1.5				+(3,3)	+	+
(2,3)	1.3		0.2	-0.2		+	+	-
(2,4)	1.7			0.2		+(3,4)	-	-
(2,5)	-2.5	1.4				-(3,5)	-	+
(3,3)	-2.1	3.3		-0.3	0.7	+(2,2)	+	+
(3,4)	1.7	0.2		0.2		+(2,4)	-	+
(3,5)	2.5			0.3		-(2,5)	-	-
(4,4)	1.6	1.2	-0.3	-0.3	-0.3	+	+	+
(4,5)				-0.1		-	+	-
(5,5)	3.1	-0.7	-0.2			+	+	+

TABLE I: hopping integrals $t(\Delta x, \Delta y; \mu, \nu)$ in units of 0.1eV. $[\Delta x, \Delta y]$ denotes the in-plane hopping vector, and (μ, ν) the orbitals. σ_y , I , and σ_d corresponds to $t(\Delta x, -\Delta y; \mu, \nu)$, $t(-\Delta x, -\Delta y; \mu, \nu)$, $t(\Delta y, \Delta x; \mu, \nu)$, respectively, where ‘ \pm ’ and ‘ $\pm(\mu', \nu')$ ’ in the row of (μ, ν) mean that the corresponding hopping is equal to $\pm t(\Delta x, \Delta y; \mu, \nu)$ and $\pm t(\Delta x, \Delta y; \mu', \nu')$, respectively. This table, combined with the relation $t(\Delta x, \Delta y; \mu, \nu) = t(-\Delta x, -\Delta y; \nu, \mu)$, gives all the in-plane hopping integrals ≥ 0.01 eV up to fifth neighbors.

In Fig.2(b), the Fermi surface for $n = 6.1$ (corresponding to $x = 0.1$) is shown in the two-dimensional unfolded BZ. For simplicity we ignore the inter-layer hopping integrals. The Fermi surface consists of four pieces (pockets in 2D): two concentric hole pockets (denoted as α_1, α_2) centered around $(k_x, k_y) = (0, 0)$, two electron pockets around $(\pi, 0)$ (β_1) or $(0, \pi)$ (β_2), respectively. α_i (β_i) corresponds to the Fermi surface around the ΓZ (MA) line (in the original BZ) in the first-principles band calculation. [14, 15, 17, 22]

Having constructed the model, we now move on to the RPA calculation. We again adopt the two-dimensional model in which the inter-layer hoppings are neglected. For the many-body part of the Hamiltonian, we consider the standard interaction terms that comprise the intra-orbital Coulomb U , the inter-orbital Coulomb U' , the Hund’s coupling J , and the pair-hopping J' . All the calculation is done in the orbital representation. Details of the multiorbital RPA calculation can be found in e.g. ref.[23]. In the present five-band case, the Green’s function is a 5×5 matrix, while the spin and the orbital susceptibility become 25×25 matrices. 32×32 k -point meshes and 1024 Matsubara frequencies are taken in the actual calculation. The Green’s function and susceptibilities are plugged into the linearized Eliashberg equation, and the gap function in a 5×5 matrix form along with the eigenvalue λ is obtained. T_c corresponds to the temperature where λ reaches unity. In the following, we present the largest eigenvalue of the spin and orbital susceptibility matrices for $i\omega_n = 0$ as $\chi_s(\mathbf{k})$ and $\chi_c(\mathbf{k})$, respectively. The gap function matrix at the lowest Matsubara fre-

quency is transformed into the band presentation by a unitary transformation. The gap for band i is presented as $\phi_i(\mathbf{k})$.

Before we proceed to the result, we can note, physically, that the characteristic Fermi surface (Fig.2) has a very suggestive form from the viewpoint that in the pairing mediated by spin fluctuations, the sign of the gap is determined so as to satisfy

$$\phi_i(\mathbf{k})\phi_j(\mathbf{k} + \mathbf{Q}) < 0 \quad (2)$$

on the Fermi surface, where \mathbf{Q} is the nesting vector around which the spin fluctuations develop. In fact, we find that the spin fluctuations dominate over orbital fluctuations as far as $U > U'$, so we can first focus on the spin structure. Let us then look at the result for χ_s for $U = 1.2$, $U' = 0.9$, $J = J' = 0.15$, and $T = 0.02$ (all in units of eV) in Fig.3(a). The spin susceptibility has peaks around $(k_x, k_y) = (\pi, \pi/2)$, $(\pi/2, \pi)$ and $(\pi, 0)$, $(0, \pi)$. This in fact reflects the Fermi surface in Fig.2(b), where we have three kinds of nesting vector: $\sim (\pi, 0)$ between α and β , and $\sim (\pi, \pi/2)$, $\sim (\pi, \pi)$ between β_1 and β_2 . A good nesting enhances tendency towards magnetism. In the RPA (where the self energy correction in the Green’s function is neglected), we have to take U as small as 1.2eV to ensure magnetic ordering does not dominate superconductivity in the temperature range considered.

For superconductivity, we show in Fig.3(c)(d) the gap function for bands three and four (as counted from below), together with the Fermi surfaces of each band. At this temperature ($T = 0.02$), the eigenvalue of the Eliashberg equation is $\lambda = 0.96$. [24] The gap is basically s -wave, but changes sign across the Fermi surfaces of band three (α_2) (and also band two; α_1 , not shown) and those of band 4 (β_1, β_2), namely, across the nesting vector $\sim (\pi, 0)$, $(0, \pi)$ at which the spin fluctuations develop, which indeed conform to the condition (2). Such a sign change of the gap between inner hole and outer electron Fermi pockets is analogous to those in models studied by Bulut *et al.*, [26] and also by two of the present authors, where T_c can be elevated because the sign change is realized without the nodes intersecting the Fermi surface. [27, 28] It is also reminiscent of the unconventional s -wave pairing mechanism for $\text{Na}_x\text{CoO}_2 \cdot y\text{H}_2\text{O}$ [29] proposed by four of the present authors. [30] After completion of the present study, we have come to notice that a recent preprint by Mazin *et al.* also concludes an s -wave pairing in which the gap changes sign between α and β Fermi surfaces. [31] However, a difference in the present case lies in the fact that the gap changes sign within the β as well. This is because of the spin fluctuations arising from the β_1 - β_2 nesting, which favors a sign change across the nesting vector $\sim (\pi, \pi/2)$ and $\sim (\pi, \pi)$. The importance of β_1 - β_2 nesting is further confirmed in our preliminary fluctuation exchange (FLEX) calculation [32], which takes account of the self-energy corrections. There we find that

χ_s takes its maximum at (π, π) rather than $\sim (\pi, 0)$ for $U = 2$, $U' = 1.3$, $J = J' = 0.35$, $n = 6.1$ and $T = 0.02$.

So we can summarize that the pairing symmetry is dominated by the presence of multiple nestings (between α - β and β_1 - β_2 in the present case). The situation is reminiscent of a three-dimensional case of disconnected Fermi surface, where the presence of intra- and inter-pocket nestings dominates the pairing symmetry.[25] While an extended s -wave gap is obtained in the present case, if the β_1 - β_2 nestings were not effective, the simplest form of the gap would be the fully-gapped extended s -wave shown in the left panel of Fig.3(b). [26, 27, 28, 30, 31]. We have found that this will be the case if $U' \simeq U$. If the α Fermi surfaces are absent, on the other hand, then the simplest form of the gap that satisfies the condition (2) would be the “fully-gapped $d_{x^2-y^2}$ ” (d_{XY} in the original BZ) (i.e., a full gap on each Fermi pocket), where the gap changes sign *between* β_1 and β_2 Fermi surfaces as shown in the right panel of Fig.3(b). To check this, we have performed RPA calculation on (i) the present model with $n = 6.3$ and (ii) a tight-binding band where we artificially shift the crystal field splitting to let the α Fermi surfaces disappear for $n = 6.1$. In both cases, we indeed obtain the $d_{x^2-y^2}$ -wave. Hence we conclude, at the present stage, that, while we have obtained the extended s -wave gap with nodes on the β Fermi surfaces, we cannot completely rule out the possibility of fully-gapped extended s - or d -wave pairings taking place because of, e.g, some modification in the band structure due to doping and/or electron correlation.

Many other interesting problems remain for future studies. Spin/orbital fluctuations and superconductivity should be studied by taking into account the self-energy correction, for which a FLEX study is underway as mentioned. It is also intriguing to investigate whether the present extended s -wave gap can quantitatively account for the specific-heat and point-contact conductance results. Also, an insight, in terms of the present model, into the origin of the high T_c superconductivity in $\text{LaO}_{1-x}\text{F}_x\text{FeAs}$ as opposed to $\text{LaO}_{1-x}\text{F}_x\text{FeP}$, [4] or LaONiP . [5]

We are grateful to Hideo Hosono for fruitful discussions and providing us with the lattice structure data prior to publication. RA is grateful to Kazuma Nakamura for discussions on the Wannier orbitals. Numerical calculations were performed at the facilities of the Information Technology Center, University of Tokyo, and also at the Supercomputer Center, ISSP, University of Tokyo. This study has been supported by Grants-in-Aid for Scientific Research from the Ministry of Education, Culture, Sports, Science and Technology of Japan, and from the Japan Society for the Promotion of Science.

-
- [1] Y. Kamihara *et al.*, J. Am. Chem. Soc. **130**, 3296 (2008).
 - [2] B.I. Zimmer *et al.*, J. Alloys Compd. **229**, 238 (1995).
 - [3] P. Quebe, L.J. Terbüchte, and W.J. Jeitschko, J. Alloys Compd. **302**, 70 (2000).
 - [4] Y. Kamihara *et al.*, J. Am. Chem. Soc. **128**, 10012 (2006).
 - [5] T. Watanabe *et al.*, Inorg. Chem. **46**, 7719 (2007).
 - [6] G.F. Chen *et al.*, unpublished (arXiv: 0803.0128)
 - [7] G. Mu *et al.*, unpublished (arXiv:0803.0928)
 - [8] L. Shan *et al.*, unpublished (arXiv: 0803.2045)
 - [9] C.-R. Hu, Phys. Rev. Lett. **72**, 1526 (1994).
 - [10] Y. Tanaka and S. Kashiwaya, Phys. Rev. Lett. **74**, 3451 (1995).
 - [11] S. Kashiwaya and Y. Tanaka, Rep.Prog. Phys. **63**, 1641 (2000).
 - [12] T. Löfwander, V.S. Shumeiko, and G. Wendin, Supercond. Sci. Technol. **14**, R53 (2001).
 - [13] X. Zhu *et al.*, unpublished (arXiv:0803.1288)
 - [14] S. Lebegue, Phys. Rev. B **75**, 035110 (2007).
 - [15] D.J. Singh and M.-H. Du, unpublished (arXiv: 0803.0429).
 - [16] K. Haule, J.H. Shim and G. Kotliar, unpublished (arXiv: 0803.1279).
 - [17] G. Xu *et al.*, unpublished (arXiv: 0803.1282).
 - [18] L. Boeri, O.V. Dolgov, and A.A. Golubov, unpublished (arXiv: 0803.2703).
 - [19] S. Baroni *et al.*, <http://www.pwscf.org/>. Here we adopt

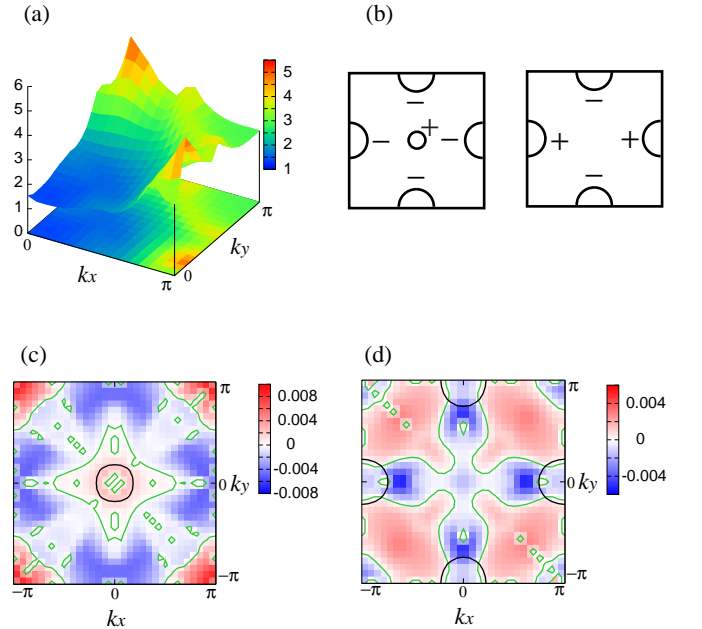


FIG. 3: RPA results for the spin susceptibility χ_s (a) and the gap function ϕ_3 (c) and ϕ_4 (d) in the band representation for $U = 1.2$, $U' = 0.9$, $J = J' = 0.15$, $n = 6.1$ and $T = 0.02$ (in eV). The black (green) solid lines represent the Fermi surfaces (gap nodes). In (b), schematic figure of the fully gapped extended s - (left) and $d_{x^2-y^2}$ -wave gaps are shown.

- the exchange correlation functional introduced by J. P. Perdew, K. Burke, and Y. Wang (Phys. Rev. B **54**, 16 533 (1996)), and the wave functions are expanded by plane waves up to a cutoff energy of 40 Ry. 10^3 k -point meshes are used with the special points technique by H.J. Monkhorst and J.D. Pack (Phys. Rev. B **13**, 5188 (1976)).
- [20] N. Marzari and D. Vanderbilt, Phys. Rev. B **56**, 12847 (1997); I. Souza, N. Marzari and D. Vanderbilt, Phys. Rev. B **65**, 035109 (2002). The Wannier functions are generated by the code developed by A. A. Mostofi *et al.*, (<http://www.wannier.org/>).
- [21] There is an ambiguity in unfolding the BZ: the sign of the hoppings $t(\Delta x, \Delta y; \mu, \nu)$ with $\Delta x + \Delta y = \text{odd}$ (i.e., hoppings between A and B sites in a bipartite lattice) is changed, a band structure is reflected with respect to $|k_x| + |k_y| = \pi$. This is just a unitary transformation, and both of the five-band structures give the same ten bands in the folded BZ, and the RPA calculation results are also unaffected.
- [22] Actually, for the undoped case, there is also a three dimensional pocket around the Z point in the original band calculation, which in the present model appears as a cylindrical Fermi surface around (π, π) at $n = 6.0$ when the out-of-plane hoppings are neglected.
- [23] T. Takimoto, T. Hotta, and K. Ueda, Phys. Rev. B **69**, 104504 (2004).
- [24] The λ value should be reduced if the self-energy corrections are considered as in FLEX.
- [25] S. Onari *et al.*, Phys. Rev. B **65**, 184525 (2002).
- [26] N. Bulut, D.J. Scalapino, and R.T. Scalettar, Phys. Rev. B **45**, 5577 (1992).
- [27] K. Kuroki and R. Arita, Phys. Rev. B **64**, 024501 (2001).
- [28] K. Kuroki, T. Kimura nad R. Arita, Phys. Rev. B **66**, 184508 (2002).
- [29] K. Takada, Nature **422**, 53 (2003).
- [30] K. Kuroki *et al.*, Phys. Rev. B **73**, 184503 (2006).
- [31] I.I. Mazin *et al.*, unpublished (arXiv:0803.2740).
- [32] N.E. Bickers, D.J. Scalapino, and S.R. White, Phys. Rev. Lett. **62**, 961 (1989).